ISSN: 1992-8645 www.jatit.org E-ISSN: 1817-3195

UNPRECEDENTED HARMONY SEARCH OPTIMIZATION-BASED LEACH ROUTING PROTOCOL (UHSO-LRP) FOR ENHANCING WIRELESS BODY AREA NETWORKING (WBAN) LIFETIME

S.VEERARATHINAKUMAR [1], Dr. B.DEVANATHAN[2]

[1] **Research Scholar, Department of Computer and Information Science, Annamalai University,** India

[2]**Assistant Professor, Department of Computer and Information Science, Annamalai University,** India

E-mail: vkumar66gee@gmail.com, devacisau@gmail.com

ABSTRACT

Wireless Body Area Networks (WBANs) play a crucial role in healthcare applications by enabling continuous and non-invasive monitoring of patients' vital signs and health data through wearable devices. These networks transmit real-time data from wearable sensors to a central monitoring system, enabling remote patient monitoring and timely medical intervention. Routing in WBANs is a critical aspect as it involves the selection of optimal paths for data transmission among various wearable devices and the central node. Traditional routing protocols face challenges in WBANs due to the characteristics of the human body, such as dynamic channel conditions, varying distances between devices, and energy constraints of wearable devices. Conventional routing protocols may not efficiently handle these issues, leading to suboptimal performance, increased energy consumption, and limited network lifetime. The proposed work, Unprecedented Harmony Search Optimization-Based LEACH Routing Protocol (UHSO-LRP), aims to address the issues faced in routing within WBANs. It introduces a hybrid approach that combines the Harmony Search Optimization (HSO) algorithm with the Low-Energy Adaptive Clustering Hierarchy (LEACH) routing protocol. The working mechanism of UHSO-LRP involves the utilization of the HSO algorithm to optimize the selection of cluster heads and the routing of data packets. The HSO algorithm introduces self-optimizing capabilities, allowing the network to dynamically adjust its configuration to changing conditions. UHSO-LRP effectively manages energy consumption and prolongs the network lifetime by optimizing the cluster head selection and data routing. Simulations are conducted to evaluate the performance of UHSO-LRP compared to conventional routing protocols. The simulations analyze key performance metrics, such as network lifetime, energy efficiency, packet delivery ratio, and latency. The results demonstrate that UHSO-LRP outperforms traditional routing protocols, showcasing significant network stability and energy utilization improvements.

Keywords: *Wireless Body Area Networks (WBANs), Routing Protocol, Harmony Search Optimization (HSO), Low Energy Adaptive Clustering Hierarchy (LEACH), Wireless Sensor Networks (WSN), Healthcare Monitoring*

1. INTRODUCTION

Wireless Body Area Networks (WBANs) are recognized as a specialized form of Wireless Sensor Networks (WSNs) specifically designed to cater to healthcare applications [1]. WBANs utilize miniature, battery-powered devices on or inside the human body to monitor vital signs and facilitate timely medical interventions. Energy conservation becomes crucial in WBANs to maximize the network's lifetime and ensure uninterrupted monitoring. Energy-efficient routing plays a pivotal role in WBANs, aiming to minimize energy consumption while maintaining reliable and efficient communication among the network's nodes [2]. As a specialized form of WSNs, WBAN routing protocols need to be energy-aware, considering the devices' limited power resources. By incorporating energy factors into routing decisions, these protocols optimize data transmission routes, balance energy consumption across devices, and utilize sleep modes to conserve energy during idle periods [3].

The energy constraints in WBANs present unique challenges compared to other WSNs or ad hoc networks. WBAN nodes are typically attached to or implanted within the human body, making frequent

ISSN: 1992-8645 www.jatit.org E-ISSN: 1817-3195

battery replacements or recharging impractical. Consequently, energy-efficient routing protocols must operate under stringent energy limitations, maximizing the network's lifetime while meeting healthcare applications' stringent quality of service (QoS) requirements [4]. One of the primary objectives of energy-efficient routing algorithms in WBANs is to balance energy consumption across nodes. Since nodes may have different energy levels, routing decisions consider the remaining energy of the nodes to distribute the energy load evenly. The network's lifetime can be extended by achieving load balancing, ensuring all nodes have sufficient energy resources to operate until the desired monitoring duration is achieved [5].

Optimizing data transmission routes is another crucial aspect of energy-efficient routing in WBANs. Traditional routing protocols that focus solely on shortest paths or congestion avoidance may not be suitable for the unique characteristics of WBANs. Instead, routing decisions must consider the energy costs associated with data transmission [6]. Energy-efficient routing algorithms aim to find routes that minimize total energy consumption while satisfying the communication requirements of the application. These algorithms consider signal strength, interference, and transmission distance to determine energy-efficient routes [7]. Sleep modes play a vital role in conserving energy in WBANs.

Given that WBAN nodes may spend significant time idle, energy-efficient routing protocols can exploit sleep modes to conserve energy during these periods. Nodes can be scheduled to enter sleep mode when they are not actively involved in data transmission or reception. By synchronizing the sleep schedules of nodes, the overall energy consumption of the network can be significantly reduced, effectively prolonging the network's lifetime [8].

Several energy-efficient routing algorithms have been proposed for WBANs, each offering advantages and trade-offs. These algorithms optimize energy consumption using clustering, data aggregation, and duty-cycling techniques. Some algorithms focus on load balancing and route selection, while others adapt routing decisions based on nodes' changing energy levels, considering the network's dynamic nature [9]. Energy-efficient routing is critical in WBANs, a subtype of WSNs tailored explicitly for healthcare applications. By incorporating energy awareness into routing protocols, WBANs can effectively balance energy consumption, optimize data transmission routes, and utilize sleep modes to conserve energy during idle periods. Developing efficient and robust energy-efficient routing algorithms remains a critical research area, enabling advancements in WBAN technology and improving patient care [10].

1.1. Problem Statement:

WBANs are specialized WSNs designed for healthcare applications. The limited energy resources of WBAN devices present challenges in ensuring network longevity and efficiency. The problem lies in developing energy-efficient routing protocols that balance energy consumption across nodes, optimize data transmission routes, and conserve energy during idle periods. Existing routing protocols may overlook the energy factor, leading to uneven energy consumption and premature battery depletion. The unique characteristics of WBANs, such as the inability to frequently replace or recharge batteries, require routing algorithms that operate under stringent energy limitations while meeting QoS requirements. Hence, developing efficient and robust energy-aware routing protocols is essential to prolong the network's lifetime, ensure reliable communication among WBAN nodes, and enhance healthcare monitoring systems' overall performance.

1.2. Motivation

The motivation behind developing energy-efficient routing algorithms for WBANs stems from the need to address healthcare applications' unique energy constraints and requirements. WBAN devices are typically battery-powered and may be attached or implanted within the human body, making frequent battery replacements or recharging impractical. Thus, energy conservation becomes crucial to extend the network's lifetime and ensure continuous and reliable healthcare monitoring. By optimizing energy consumption, balancing the energy load across nodes, and leveraging sleep modes during idle periods, energy-efficient routing protocols can significantly enhance the efficiency and longevity of WBANs. Efficient energy-aware routing algorithms reduce maintenance costs, improve patient safety, and enable uninterrupted monitoring of vital signs. Developing energy-efficient routing protocols in WBANs aims to maximize the network's lifetime, enhance overall system performance, and improve the quality of healthcare services provided through WBAN technology.

1.3. Objective

The primary objective of this research is to develop energy-efficient routing algorithms for Wireless Body Area Networks (WBANs) in healthcare applications. The main focus is to optimize energy consumption, prolong the network's lifetime, and improve overall system performance. Specific objectives include:

- Balancing Energy Consumption: Design routing protocols that distribute the energy load evenly across WBAN nodes, considering variations in their energy levels. This objective aims to prevent premature battery depletion and ensure all nodes have sufficient energy resources for uninterrupted operation.
- Optimizing Data Transmission Routes: Develop routing algorithms that consider energy costs associated with data transmission, considering factors such as signal strength, interference, and transmission distance. The objective is to find routes that minimize energy consumption while satisfying communication requirements.
- Energy Conservation during Idle Periods: Implement sleep modes in the routing protocols to conserve energy during periods of inactivity. Synchronize sleep schedules among nodes to minimize energy consumption while ensuring timely data transmission when required.

Adhering to QoS Requirements: Ensure that the developed routing algorithms meet the stringent QoS requirements of healthcare applications, such as the timely and reliable transmission of vital signs data.

2. LITERATURE REVIEW

"Cooperative WBAN Performance Evaluation" [11] involves assessing the system's performance metrics and optimizing energy utilization. Through simulations, it analyzes factors such as communication reliability, latency, and network capacity to evaluate the system's effectiveness under different scenarios. It aims to maximize energy efficiency by reducing power consumption at various levels, such as sensor nodes, communication protocols, and resource management strategies. "TransGA" [12] is designed for intra-WBAN communication. TransGA utilizes Genetic Algorithms (GA) to optimize the transmission parameters and strategies within the network, including power allocation, channel selection, modulation schemes, and coding schemes. "NeoHeartNet" [13] revolutionizes early congenital heart defect diagnosis in neonates. By leveraging wearable devices and sensors in the first tier, NeoHeartNet collects vital signs and physiological data from newborns. The second tier comprises a cloud-based processing and analysis platform that receives and analyzes the data to detect potential heart defects. The third tier involves a network of specialized healthcare professionals who receive the analyzed data for expert diagnosis and recommendations. "EnerWBAN" [14] maximizes energy utilization and efficiency by employing adaptive power management, duty cycling, optimal resource allocation, and energy-aware routing protocols. These methods enable efficient utilization of ambient energy sources, prolong sensor node battery life, and ensure sustainable and long-term monitoring.

"RelayStar" [15] enhances the performance of IEEE 802.15.6-based two-hop star topology WBANs. RelayStar intelligently selects the most suitable relay nodes to improve communication reliability and network efficiency by considering signal quality, channel conditions, and energy levels. "HarvestComm" [16] revolutionizes communication optimization in such networks. By utilizing reinforcement learning algorithms, HarvestComm learns and adapts communication strategies based on the available harvested energy, network conditions, and communication requirements. It explores the solution space to identify the most effective actions, including transmission power and channel selection. "PowerECG Node" [17] is designed to perform real-time feature extraction in WBANs. PowerECG Node optimizes power consumption while efficiently processing ECG (Electrocardiogram) signals. It incorporates power management techniques like power gating, voltage scaling, and dynamic and frequency scaling. "DeepBANTrans" [18] is designed specifically for WBANs based on the IEEE 802.15.6 standard. DeepBANTrans leverages the power of deep learning techniques to enhance the performance of the baseband transceiver, enabling reliable and efficient communication through the human body. Optimization plays significant role in all kinds of networking [19]–[38], [39].

"StableLink" [40] was designed to enhance the stability period in WBANs. By leveraging energy-aware metrics and reliability factors, StableLink optimizes routing paths to prolong stability, ensuring continuous and uninterrupted network connections. It employs dynamic route maintenance, fault tolerance mechanisms, and adaptive routing protocols to adapt to changing network conditions and node failures. "FaultAI-WBAN" [41] is a fault prediction framework designed for WBANs. By harnessing the power of advanced machine learning techniques, FaultAI-WBAN analyzes historical data to identify patterns and predict potential faults or failures within the WBAN system. Through supervised learning, deep learning, or ensemble methods, the framework learns from past fault instances and develops predictive models that can anticipate future failures. "CoopUWB-Opti" [42] focuses on maximizing the efficiency and reliability of communication within CM3A cooperative WBANs by leveraging UWB technology. This approach employs optimization techniques, including resource allocation, power control, and interference management, to effectively utilize the UWB spectrum. "SDN-EnergyRoute" [43] aims to optimize the routing process in WBANs to maximize energy efficiency and network performance. By leveraging the principles of SDN, the algorithm centralizes network control and enables dynamic and intelligent routing decisions. SDN-EnergyRoute considers energy consumption, link quality, and network congestion to determine the most energy-efficient and reliable routing paths.

"AnonyAuth-WBAN" [44] focuses on lightweight implementation while ensuring mutual authentication between the wearable devices and the WBAN infrastructure. AnonyAuth-WBAN employs cryptographic techniques to establish secure communication channels and protect user identities from unauthorized access. The scheme enables wearable devices to authenticate without revealing sensitive information by incorporating anonymous authentication mechanisms. "MaxMinPower-WBAN" [45] focuses on optimizing power control strategies to ensure efficient and reliable communication within the network. MaxMinPower-WBAN aims to maximize the minimum received signal power among all nodes in the network by dynamically adjusting transmission power levels. It considers the distributed nature of WBANs, where wearable devices operate nearby. "IM-QRP" [46] aims to enhance QoS by optimizing the routing process within the network. By considering various factors such as energy consumption, network congestion, and link quality, IM-QRP intelligently selects the most efficient routes for data transmission. The protocol prioritizes QoS metrics such as packet delivery ratio and latency.

"Congestion Control Aware Routing Algorithm (CCARA)" [47] is a cutting-edge routing algorithm designed for Software Defined WBANs with a focus on energy efficiency and congestion control. CCARA aims to optimize data routing in WBANs while considering temperature variations by considering energy consumption and network congestion. The algorithm dynamically adjusts routing paths based on real-time temperature measurements to minimize energy consumption and avoid congested areas. "Energy-efficient Harvest-Aware Routing Protocol (E-HARP)" [48] addresses energy efficiency in WBANs by incorporating harvested energy awareness into the clustering and routing process. The protocol actively promotes the formation of energy-efficient clusters by considering the availability of harvested energy from wearable devices. E-HARP ensures optimal utilization of energy resources by actively selecting energy-efficient cluster heads and employing cooperative routing strategies.

3. PROPOSED WORK

3.1. LEACH

Popular hierarchical routing protocol LEACH (Low Energy Adaptive Clustering Hierarchy) was designed for WSNs. Its primary goal is to reduce energy use in WSNs by dividing the network into smaller groups and rotating nodes through the position of cluster leader. This methodology guarantees a well-balanced distribution of energy consumption across the entire network.

3.1.1. Cluster Formation

During the cluster formation phase, the network is partitioned into clusters, each overseen by a designated cluster head. The selection of cluster heads is determined by a probabilistic model, wherein nodes decide to become either a cluster head or a regular member based on a predefined threshold value.

3.1.2. Calculation of the Probability of Becoming a Cluster Head

To achieve a balanced distribution of energy consumption, every node calculates its probability of becoming a cluster head, represented as $p(i)$, using Eq.(1a).

$$p(i) = \left(P / \left(1 - P * \left(r \bmod (1/p)\right)\right)\right) \text{ if } G(i) \quad 0 \text{ if } G(i) = 0 \tag{1a}$$

where P indicates Optimal network composition based on the number of cluster leaders, r indicates the present round, $G(i)$ denotes the Binary indicator function representing node i (0 if it is not a cluster head, 1 otherwise). The probability $p(i)$ is determined by taking into account the desired percentage of cluster heads in the network and the current round. Each node calculates its probability based on its state (whether it is currently a cluster head or a regular node).

3.1.3. Cluster Head Selection

After calculating the probabilities, each node i generates a random number, rand(i), uniformly distributed between 0 and 1. If rand(i) is less than or equal to p(i), the node becomes a cluster head; otherwise, it remains a common node. Once the cluster heads are selected, they broadcast their information to the entire network. Ordinary nodes determine which cluster to join based on the signal strength they receive from the cluster heads. This helps in creating efficient and localized communication within each cluster.

3.1.4. Data Transmission

During the data transmission phase, the cluster heads gather data from their member nodes, aggregate it, and transmit it to the base station. This aggregation reduces the overall communication overhead and conserves energy. The energy consumed by node i during data transmission, denoted as $Etx(i)$, and the energy consumed by node i during data reception, denoted as $ERx(i)$, can be represented by Eq.(1b).

$$E(i) = Etx(i) + ERx(i) \tag{1b}$$

Efficient data transmission and reception strategies are employed to minimize energy consumption during these processes.

3.1.5. Cluster Head Rotation

To achieve a balanced distribution of energy consumption across the network, the cluster heads periodically rotate their roles. After completing a round, all nodes become regular nodes, and the cluster head selection process is repeated. This rotation ensures that energy is evenly distributed across the network, preventing specific nodes from depleting their energy resources quickly. Employing the LEACH protocol can significantly improve energy efficiency in wireless sensor networks, extending the network's lifetime. The protocol achieves this by dynamically selecting cluster heads based on probabilistic calculations, organizing the network into clusters, aggregating data, and rotating the cluster head roles. The distributed nature of the protocol reduces energy consumption and increases the overall network lifetime.

It is important to note that the equations and variables provided are general representations of the LEACH protocol. The specific implementation details and parameters may vary depending on the protocol's variant or version. Researchers and network designers can customize and fine-tune these parameters based on the specific requirements and characteristics of the wireless sensor network deployment.

Algorithm 1: LEACH
Step 1: Initialization Set desired CH percentage and assign random numbers to nodes. **Step 2: Cluster Head Selection** Nodes compare random numbers with the threshold to become CHs. **Step 3: Cluster Formation** The signal intensity at each node determines which CH it will join.

ISSN: 1992-8645 www.jatit.org E-ISSN: 1817-3195

Step 4: Data Transmission

Ordinary nodes transmit data to their respective CHs.

Step 5: Data Aggregation and Transmission

CHs aggregate and transmit data to the base station.

Step 6: Energy Dissipation and Rotation

Nodes estimate energy and decide CH's role for the next round.

Step 7: Repeat steps 2 to 6 for multiple rounds to optimize energy consumption and network lifetime.

3.2. Unprecedented Harmony Search Optimization (UHSO)

3.2.1. Harmony Search Algorithm

The Harmony Search Algorithm (HSA) is a powerful and innovative technique for efficiently solving complex optimization problems. Inspired by achieving perfect harmony in music, the HS algorithm aims to find optimal solutions by mimicking the search for optimal musical harmony. This approach has proven highly effective in tackling many real-world problems. At the core of the HSA lies a population-based mechanism known as "harmony memory" (HM). Like other meta-heuristic search methods, the HM is a repository of potential solutions. The capacity of this HM and the processing speed with which it operates are crucial control parameters that significantly impact the algorithm's performance.

Two additional essential parameters in the HS algorithm are the HM consideration rate (HMCRω) and the pitch adjusting rate (PARω), both of which lie within the range [0, 1]. The HMCRω determines the selection probability of a decision variable present in HM, which allows the algorithm to exploit promising solutions. On the other hand, the PARω controls the rate at which the decision variables are adjusted during the search, promoting exploration of the solution space. The HS algorithm can be divided into five primary stages:

Step 1: Initialization: The process starts by initializing the HM with random solutions, often within predefined bounds for each decision variable.
Step 2: Improvisation: In this stage, the algorithm creates a new harmony by generating candidate solutions. Each decision variable value in the new harmony is determined by drawing from the HM with a probability given by HMCRω or by generating a random value within the variable's domain. This process balances exploiting existing reasonable solutions and exploring new regions of the solution space.
Step 3: HM Update: After generating a new harmony, its fitness or objective value is evaluated. If the new harmony performs better than any existing one in the memory, it replaces the worst harmony in the set. This constant refinement process enables the algorithm to improve the solutions over time.
Step 4: Iteration: Steps 2 and 3 are iteratively performed a predefined number of times or until a termination criterion is met. With better solutions, the HM is updated during each iteration, and the search process becomes more focused on promising regions of the solution space.
Step 5: Termination: The algorithm gets terminated with the predefined iteration count is reached or when a specific termination condition, such as a satisfactory level of convergence or solution quality, is achieved.

By effectively combining the principles of musical harmony with an intelligent search mechanism, the HSA has proven to be a robust and versatile optimization technique capable of finding high-quality solutions in various problem domains. Its ability to balance exploration and exploitation makes it well-suited for solving complex problems with numerous local optima, where other traditional optimization methods may struggle. As a result, the HSA continues to be a valuable tool in diverse fields, including engineering, finance, logistics, and many others.

3.2.2. Parameter Setting

The optimization objective is to minimize the objective function $g(p)$ concerning the decision vector $p = (p_1, p_2, \dots, p_r)$. The function $g(p)$ represents the problem-specific objective function, which maps the decision variables to a real-valued scalar to be minimized. In mathematical notation:

$$min_p \; g(p) \tag{2a}$$

ISSN: 1992-8645 www.jatit.org E-ISSN: 1817-3195

where 'p' is the decision vector and '$g(p)$' returns the objective function value for the given vector 'p'.

To address the optimization problem, this research considers the search space Ω, defined as the product space of Y decision axes:

$$\Omega = \prod_{w=1}^{Y} [Z_w, O_w] \qquad (2b)$$

where Z_w and O_w represent the lowest and highest values for the w-th decision axis, respectively.

The Harmony Search Algorithm (HSA) operates based on a population of harmony vectors, which are candidate solutions represented as $p = (p_1, p_2, \ldots, p_Y)$. The algorithm aims to iteratively refine these harmony vectors to improve the quality of solutions and converge towards the optimal solution that yields objective function $g(p)$ with the lowest value.

The Initialization of the Harmony Search algorithm involves setting various parameters:

- **Search Radius Control Parameter (bandwidth mn):** The search radius control parameter mn influences the search space exploration. It determines the width of the neighbourhood around a harmony vector within which new solutions can be generated. An enormous mn value encourages more extensive exploration, while a smaller value narrows the search area, focusing on local regions.
- **Improvisation Control Parameter (ICP):** The improvisation control parameter ICP governs the probability of introducing random values during the search. A new harmony vector is generated randomly at each iteration, with a probability of ICP. Higher values of ICP promote greater random exploration, while lower values enhance the exploitation of the existing harmony vectors.
- **Size of HM (SHM):** It determines the population or set of potential solutions the algorithm explores and refines to find the optimal solution to the optimization problem. These harmony vectors store the best solutions so far and serve as the basis for generating new solutions.
- **HM Consideration Rate ($HMCR$):** The HM consideration rate HMCR determines the probability of selecting values from the HM when generating a new harmony vector. A higher value of $HMCR$ increases the likelihood of choosing values from memory, leading to greater exploitation of promising solutions.
- **Pitch Adjustment Rate (PAR):** The pitch adjustment rate PAR controls the degree of change applied to each decision variable during forming a new harmony vector. It directly affects the diversity of solutions generated at each iteration. A higher value of PAR promotes more extensive exploration, while a lower value focuses on exploiting the neighbourhood around existing solutions.

The default values of $SHM, mn, ICP, HMCR,$ and PAR are set initially to balance exploration and exploitation. During optimization, these parameter values can be adjusted based on the problem's characteristics to enhance the algorithm's performance and facilitate convergence towards the optimal solution. HSA iteratively generates and evaluates new harmony vectors until a termination criterion is met. The best solution in the HM represents the optimized values of the decision variables, minimizing the objective function $g(p)$.

3.2.3. HM Initialization

The HS algorithm begins by initializing the HM, a collection of harmony vectors representing potential solutions to the optimization problem. The parameter HMS is analogous to the population size in other meta-heuristic algorithms.

(a). Harmony Vector Representation

A harmony vector p_{sw} represents a potential solution, where $s = 1, 2, \ldots, HMS$, denotes the harmony vector index present in the memory, and $w = 1, 2, \ldots, Y$, indicates a specific decision variable component of the vector.

(b). Harmony Vector Initialization

The HM is created by randomly generating HMS harmony vectors. For each component w of each harmony vector s, the value p_sw is initialized using Eq.(3).

$$p_{sw} = Z_w + (O_w - Z_w).rand(0,1) \qquad (3)$$

where p_{sw} represents the value of the w-th decision variable in the s-th harmony vector, Z_w and O_w denotes the lowest and highest value of the w-th decision variable, $rand(0,1)$ indicates a random number generator function that produces a randomly generated value that lies between 0 and 1.

(c). Search Space Definition

The search space Ω is defined in Eq.(1) are the product space of Y decision axes, where each decision axis w has a range defined by its Z_w and O_w values.

ISSN: 1992-8645 www.jatit.org E-ISSN: 1817-3195

(d). Objective Function Evaluation

After initializing the HM, the next step is to evaluate the objective function g(p) for each harmony vector in the memory. The objective function maps a decision vector $p = (p_1, p_2, \dots, p_Y)$ to a real-valued scalar, representing the fitness of the solution $g(p_{sw})$.

(e). HM Update

The HS algorithm proceeds with iterative updates to the HM. New harmony vectors will be generated and evaluated at each iteration, replacing or improving the existing memory solutions. The algorithm aims to converge towards better solutions by iteratively refining the HMS.

3.2.4. Fresh Harmony Generation

Once the HM is initialized, the HSA proceeds to create a new harmony vector, $p' = (p'_1, p'_2, \dots \dots . p'_Y)$, by applying three strategies, which are: (a) consideration of memory level, (b) adjustment of pitch, and (c) selecting random values

(a). Consideration of Memory Level

The memory consideration rule is guided by the $HMCR$ parameter. With a probability of $HMCR$, a component of the new harmony vector p' is selected from the HM. This means that some elements of p' are directly borrowed from the existing harmony vectors in the memory, promoting the exploitation of promising solutions.

(b). Adjustment of Pitch

The pitch adjustment rule is influenced by the PAR parameter. For each component p' of the new harmony vector, with a probability of $(1 - HMCR) * PAR$, a pitch adjustment is applied. The adjustment involves perturbing the value of p' based on the difference between the current component value and another randomly chosen component value from the memory. This operation encourages the exploration of the search space.

(c). Selecting Random Values

With a probability of $(1 - HMCR) * (1 - PAR)$, the random selection rule comes into play. In this case, the component p' is randomly generated within the valid range $[Z_i, O_i]$ of the i-th decision axis. This random selection introduces diversity and ensures that the algorithm explores the search space beyond the scope of the HM.

Algorithm 1: Fresh Harmony Generation

Input:

- HM: The current HM contains HMS harmony vectors.
- HMCR: To determine the probability of selecting values from the memory.
- PAR: To control the amount of change applied to each decision variable.
- Decision space Ω: The product space of Y decision axes, each with its Z_w and O_w values

Output:

- New Harmony Vector $p' = (p_1', p_2', \dots, p_Y')$

Procedure:

Step 1: Initialize an empty harmony vector $p' = (p_1', p_2', \dots, p_Y')$

Step 2: For each component $w = 1 \; to \; Y$ of p', perform the following:

a. Between 0 and 1, generate a number randomly

b. If the generated random number is less than or equal to $HMCR$, then:

- Select a value from the corresponding component w of a randomly chosen harmony vector from the HM.
- Update the component $p_i{}'$in p' with the selected value.

c. Else if the generated random number is more significant than $HMCR$ and less than or equal to $(HMCR + (1 - HMCR) * PAR)$, then:

- Choose a random harmony vector h from the memory.
- Apply pitch adjustment to the component $p_i{}'$in p' based on the difference between $p_i{}'$and the corresponding component in h.

d. Else (the generated random number is greater than $(HMCR + (1 - HMCR) * PAR)$), then:

- Randomly generate a new value for the component $p_i{}'$within the valid range $[Z_i, O_i]$.
- Update the component $p_i{}'$in $p'$with the generated value.

Step 3: Return the newly created harmony vector.

3.2.5. Termination Criterion Verification

HSA uses a termination criterion to stop generating new harmony vectors. It checks if the maximum number of iterations is reached, and if so, the algorithm ends; otherwise, it continues until the condition is met.

ISSN: 1992-8645 www.jatit.org E-ISSN: 1817-3195

Algorithm 2: Termination Criterion Verification

Input:

- Current Iteration Count: The number of iterations performed in the HS algorithm.
- Highest Iterations: The predefined highest number of iterations to terminate the algorithm.

Output:

- Termination Decision: A boolean variable indicating whether the termination criterion is met.

Procedure:

Step 1: Check if the Current Iteration Count is less than the Highest Iterations.

- If true, the criteria for termination are not reached, and the algorithm continues.
- If false, the criterion for termination is reached, and the algorithm stops.

Step 2: Return the Termination Decision.

3.2.6. Global-best HSA

HSA demonstrates remarkable proficiency in addressing numerical optimization problems by efficiently identifying high-performance regions within the solution space. However, it exhibits limitations when it comes to conducting effective local searches. This discrepancy between its potential and practical usage has led researchers to propose an enhanced version of HSA known as UHSO to rectify this weakness. Given that HSA already outperforms competing methods, the research focuses on optimizing its convergence performance through targeted adjustments. UHSO integrates a modified version of HSA while incorporating supplementary techniques to strike a balance between exploration and exploitation. Here is a comprehensive overview of these enhancements:

- **Modified HSA:** The core HSA algorithm is fine-tuned to improve its local search capabilities and overall convergence efficiency.
- **Additional Techniques:** UHSO introduces supplementary methods to augment the algorithm's ability to effectively explore and exploit the solution space.

The integration of these improvements empowers UHSO to capitalize on HSA's existing strengths while addressing its limitations, resulting in a more robust and efficient optimization approach.

(a). Initialization based on Opposition

In UHSO, an antithesis-based learning approach is employed to enhance the solution quality of the original HM. This unique approach introduces a technique that has succeeded in various meta-heuristic algorithms. The primary goal is to balance exploration and exploitation, resulting in improved convergence performance. By integrating the antithesis-based learning into the harmony search algorithm, the proposed method, referred to as UHSO, effectively addresses the limitations of the original HSA and achieves enhanced optimization efficiency. The adjustments made to the core HSA algorithm and the incorporation of supplementary techniques contribute to the overall efficacy of the UHSO approach.

Algorithm 3: Initialization using Opposition

Input:

- HMS: The size of HM, representing the number of harmony vectors.
- Y: The number of decision variables in the problem.
- Z_w: The lowest value for the w-th decision variable.
- O_w: The highest value for the w-th decision variable.

Output:

- HM: A collection of harmony vectors representing potential solutions.

Procedure:

Step 1: For each harmony vector s from 1 to HMS, do the following:

a. For each decision variable w from 1 to Y, do the following:

- Between 0 and 1, generate a number randomly.
- Calculate p_{sw}.

Step 2: For each harmony vector s from 1 to HMS, do the following:

a. For each decision variable w from 1 to Y, do the following:

- Calculate the oppositional instruction value

Step 3: Return the HM containing the initialized harmony vectors with their respective decision variable values.

(b). $F/DE/best/1$ Mutation Technique

$DE/best/1$ refers to a specific mutation strategy used in the Differential Evolution (DE) algorithm. DE is a popular optimization algorithm used for global optimization problems. It belongs to the family of evolutionary algorithms and is particularly effective in solving continuous optimization problems. In the DE algorithm, the population consists of candidate solutions called "individuals" or "vectors." These individuals are represented as vectors in the search space, and they undergo mutation, crossover, and selection processes to produce new generations. The notation "$DE/best/1$" specifies the specific mutation strategy used in DE:

- "DE": Stands for Differential Evolution, the algorithm's name.
- "$best$": Refers to the strategy that involves the selection of the best individual (solution) from the current population as a reference or base vector during the mutation process.
- "1": Signifies that only one mutant vector is generated for each population member during the mutation process.

Using fuzzy logic in the $DE/best/1$ strategy allows for a more flexible and adaptive approach in selecting the best individual and scaling factor during the mutation process. The fuzzy logic-based $DE/best/1$ (i.e., $F/DE/best/1$) is outlined in Algorithm 4.

Algorithm 4: $F/DE/best/1$	
Step 1:	For each individual in the population, utilize fuzzy logic to determine the "degree of fitness" or "closeness to the best solution" of that individual compared to the other individuals in the current generation. This degree of fitness can be represented by a fuzzy membership function, which captures the individual's proximity to the best solution in the population.
Step 2:	Based on the fuzzy membership values, identify the best individual with the highest degree of fitness as the reference or base vector for mutation. Fuzzy logic allows for a gradual transition between individuals, considering their relative fitness levels rather than strictly selecting the best individual.
Step 3:	Employ fuzzy logic to adjust the mutation factor (F) adaptively based on the individuals' fitness and problem characteristics. The fuzzy inference system can consider factors like the convergence rate, exploration-exploitation trade-off, and problem complexity to determine an appropriate mutation factor.
Step 4:	Mutate the base vector by adding the scaled difference between other individuals, guided by the fuzzy membership values and the dynamically adjusted mutation factor.
Step 5:	Create a new mutant vector using the fuzzy-guided mutation process.
Step 6:	Utilize fuzzy logic for crossover and selection. The crossover rate and the decision of whether to replace the original individual with the trial vector can be made based on fuzzy rules that consider the fitness and characteristics of both individuals.

By incorporating fuzzy logic into the DE/best/1 strategy, the base vector, mutation factor, and other parameters selection becomes more adaptive and data-driven. The fuzzy-based approach allows the algorithm to respond to changes in the problem landscape and dynamically adjust its behaviour during optimization. This adaptability enhances the exploration and exploitation capabilities of the DE algorithm, leading to improved convergence and better solutions for a wide range of optimization problems.

(c). Enhanced Improvisational Strategies

The HSA's pitch adjustment phase has limited local search capabilities, resembling more of a random search. To address this limitation, the HSA incorporates a globally best-guiding system. Additionally, the $F/DE/best/1$ mutation technique is employed to enhance HSA, leveraging the superior local search capabilities of the $F/DE/best/1/bin$ approach. Essentially, the traditional pitch-adjustment method in HSA is replaced with a variant of the $F/DE/best/1$ mutation procedure. The modified pitch-adjustment equation is given by Eq.(4):

$$p'_w = \prod p_{best,a} + \zeta.(p_{d,a} - p_{v,a}) \tag{4}$$

Here, ζ is a scale factor regulating the amplification of the differential variation $p_{d,a} - p_{v,a}$, where $w = 1, 2, \ldots, Y$. The index 'best' refers to the best harmony in the HM, and $'a'$ is a randomly chosen integer in the range $[1, Y]$. The variables $'d'$ and $'v'$

ISSN: 1992-8645 www.jatit.org E-ISSN: 1817-3195

are random integers, each taken from the set $[1, \ldots, HMS]$, and different from $'best'$, respectively.

For effective local search, a smaller value of ζ is preferable. Similarly, the random selection phase of HS also exhibits characteristics of a random search. To enhance global search capability and reduce unpredictability, a modified version of the Artificial Bee Colony (ABC) algorithm is introduced to replace the random selection equation in HS. The substitution is based on the understanding that ABC is adept at exploring new search spaces. The modified solution searching equation, replacing HS's random selection, is represented by Eq.(5):

$$p'_w = \prod p_{u,w} + \phi_w \cdot (p_{u,w} - p_{y,w}) \quad (5)$$

where w represents the decision variable index, ranging from 1 to Y. The variable u and $y$represents a number generated randomly with uniformed dispersion in the interval $[1, HMS]$, 'ϕ_w' denotes a uniformly dispersed random number within the interval $[-1, 1]$.

3.2.7. Update of HMCR and PAR

Two crucial contextual factors in HSA and its variants are HMCR and PAR. Optimizing these parameters can lead to significant improvements in both local and global solution quality. Considering the cyclic nature of natural processes, a periodic approach is adopted, selecting the three rules for improvising a new harmony at roughly periodic intervals. The sine function is well-suited for modelling such cyclic events. A sign function based on the sine function is employed to ensure that both parameter values remain non-negative. By combining these two functions, a novel function is formulated to maintain the positive nature of the parameters. The proposed time-variant techniques for the two variables, HMCR and PAR, are as follows:

(a). HMCR Update

$$HMCR(FEs) = \left(HMCR_{min} + \frac{HMCR_{max} - HMCR_{min}}{maxFEs} FEs\right) \times max\left(0, sgn(sin(FEs))\right) \quad (6)$$

where $HMCR(FEs)$ represents the rate of congruence between memory and thought during the iterative process, FEs is the variable being iterated on, $HMCR_{min}$ and $HMCR_{max}$ denote the lowest and highest HM consideration rates, sign function is represented as $sgn(.)$, and the sine function is represented as $sin(.)$.

(b). PAR Update

$$PAR(FEs) = (PAR_{min} + \frac{\frac{PAR_{max} - PAR_{min}}{maxFEs} \times FEs}{maxFEs} \times max(0, sgn(sin(FEs))) \quad (7)$$

Where $PAR(FEs)$ is the rate at which the pitch is adjusted for the iterative variable FEs. PAR_{max} and PAR_{min} represent the lowest and highest adjusting rates. By continuously updating $HMCR$ and PAR using these time-variant techniques, the HSA can adapt its parameters dynamically, leading to improved exploration and exploitation capabilities and ultimately enhancing the overall optimization performance.

Algorithm 5: Update of HMCR and PAR
Input: • FEs and $maxFEs$: The iterative variable representing the current iteration number. • $HMCR_{min}$ and $HMCR_{max}$ • PAR_{min} and PAR_{max} **Output:** • Updated HMCR and PAR values. **Procedure:** **Step 1:** Calculate the rate of congruence between memory and thought (HMCR) using Eq.(6). **Step 2:** Calculate the pitch adjustment rate (PAR) using Eq.(7). **Step 3:** Return the updated HMCR and PAR values.

3.2.8. Global Search Enhancement

After updating HMCR and PAR, UHSO incorporates two additional exploring strategies to enhance its global search capability. These strategies aim to refine the updated UHSO by introducing higher levels of exploration, especially during the early phases of the meta-heuristic algorithm development. The emphasis on exploration is crucial to prevent the algorithm from being trapped in local minima and to facilitate the search for optimal solutions. The two perturbed schemes are designed to promote diverse exploration across the solution space:

- **Highly Exploratory Strategies:** During the initial stages of the meta-heuristic algorithm's execution, it is essential to prioritize exploration to thoroughly explore the solution space and avoid converging prematurely to local minima. The first perturbed scheme focuses on highly exploratory strategies involving more extensive and radical explorations. This allows the algorithm to cover many potential solutions, increasing the chances of finding the global optimum.

- **Avoiding Local Minima:** Another critical aspect of the two perturbed schemes is to prevent the algorithm from getting stuck in local minima. Local minima are suboptimal solutions that can hinder the algorithm from reaching the global optimum. The second perturbed scheme aims to mitigate the impact of local minima by introducing techniques that encourage the exploration of unexplored regions of the solution space. This helps the algorithm break free from the influence of local optima and continue its search for more promising solutions.

The updated UHSO can balance exploration and exploitation effectively, ensuring a more comprehensive and effective global search. The algorithm's ability to navigate diverse areas of the solution space enables it to discover better solutions, even in complex and challenging optimization problems. The combination of these perturbed strategies contributes to the overall robustness and efficiency of the UHSO in finding optimal harmonies.

(a). Modification based on ABC for Optimum Harmony

In the UHSO, the perturbed scheme for achieving optimal harmony draws inspiration from the modern artificial bee concept in the ABC algorithm. Eq.(8) precisely captures the Optimal Harmony.

$$r_w = p_{best,w} + \phi_w \cdot (p_{best,w} - p_{a,w}) \quad (8)$$

where $w = 1, 2, \dots, Y$ denotes the index of the decision variable, ϕ_w represents an irrational real number between 0 and 1, introducing adaptability to the perturbation process. The variable '$best$'corresponds to the highest-rated harmony in the current HM, signifying the best solution found so far. 'a' indicates a randomly selected integer value from the range $[1, HMS]$ representing a solution other than the best. It is to be noted that 'a' is different from '$best$' to promote the exploration of diverse solutions.

The primary objective of employing the perturbation technique is to avoid getting trapped in local minima. By perturbing the best harmony, the $UHSO$ algorithm is guided to explore different regions, thus mitigating the risk of converging prematurely to suboptimal solutions.

To address this concern, a control mechanism is introduced using the percentage parameter 'δ'. This parameter governs the rate at which the improved solution search equation is integrated into the $UHSO$ algorithm. Fine-tuning the value of 'δ' allows the algorithm to balance exploration and exploitation, ensuring efficient convergence while capitalizing on the perturbation technique's ability to escape local minima.

Incorporating ABC-inspired modifications enriches the $UHSO$'s capacity to explore diverse solution spaces and efficiently identify optimal harmonies. The adaptive nature of the perturbation process, guided by the irrational real number ϕ_w, endows the algorithm with enhanced adaptability and robustness in tackling intricate and challenging optimization problems.

Algorithm 6: Modification based on ABC for Optimum Harmony

Input:
- HM: HM containing candidate solutions.
- Y: Number of decision variables.
- HMS: HM Size, representing the population.
- δ: Percentage parameter controlling the rate of perturbation (Eq. 8).
- $best_{index}$: Index of the best harmony in the current HM.
- $maxFEs$: Highest number of iterations.

Output:
- Updated harmony vector r_w.

Procedure:

Step 1: Select a random integer a from the range $[1, HMS]$, ensuring a is not equal to $best_{index}$

Step 2: Between 0 and 1, Generate an irrational real number $\phi_w$randomly.

Step 3: For each decision variable 'w' from 1 to Y, calculate the new harmony element using the ABC-inspired perturbation (i.e., Eq.(8)).

Step 4: Apply the control mechanism to regulate the perturbation process:
- Calculate the perturbation

	threshold • If the current iteration 'FEs' is less than or equal to perturb_threshold, update the harmony vector using the ABC-inspired perturbation as in step 3. Otherwise, use the standard harmony improvisation rules.
Step 5:	Return the updated harmony vector r_w.

(b). Fine-Tuning of Optimum Harmony using Opposition-Based Learning (OBL)

Incorporating an Opposition-Based Learning (OBL) perturbed scheme, the $UHSO$ aims to significantly enhance its capability to escape local minima and explore uncharted territories. The perturbation strategy is designed as Eq.(9).

$$r_w = Z_w + O_w - p_{best,w} \qquad (9)$$

where Z_w and O_w represent the lowest and highest values of component w, while $p_{best,w}$ corresponds to the element of the best harmony found in the current HM.

The OBL-based perturbation strategy is crucial in provoking dimensional disruptions in the best harmony. By systematically exploring each dimension, the algorithm gains an advantage in navigating towards unexplored regions, promoting thorough exploration, and effectively escaping local minima. To maintain a balance between exploration and exploitation, the frequency of introducing the updated solution search equation based on the OBL scheme is regulated by the carefully selected percentage parameter 'γ'. By fine-tuning 'γ', the algorithm's responsiveness to the perturbed strategy can be adjusted, allowing it to adapt its search behaviour per the problem's complexity.

Combining the OBL-inspired perturbation scheme with the ABC-based Modification enhances the UHSO algorithm with remarkable adaptability and robustness in tackling intricate optimization challenges. The algorithm's innate ability to explore a diverse solution space and its improved capacity to fine-tune optimum harmony culminate in a powerful and efficient optimization approach suitable for solving a wide range of complex real-world problems.

3.2.9. Handling Bound Constraints

To ensure practical and feasible solutions for optimization problems, it is crucial to address the bound constraints that may restrict the decision variables. Eq.(10) effectively manages bound constraints within the UHSO:

$$p_{sw} = \begin{cases} Z_w + rand(0,1).(O_w - Z_w), & \text{if } p_{sw} < Z_w, \\ O_w - rand(0,1).(O_w - Z_w), & \text{if } p_{sw} > O_w. \end{cases} \qquad (10)$$

where p_{sw} represents the value of the decision variable w in the harmony at index s. Z_w and O_w denote the lowest and highest bounds for decision variable w. $rand(0,1)$ generates a random number between 0 and 1.

The bound constraint handling mechanism ensures that the decision variable p_{sw} remains within the specified bounds, ensuring that the solutions generated during the Harmony Search process are practical and feasible. If the current value of p_{sw} falls below the lower bound Z_w, it is randomly adjusted within the range [Z_w, O_w]. Similarly, if p_{sw} exceeds the upper bound O_w, it is adjusted within the range [Z_w, O_w] using random perturbation. By incorporating this bound constraint management technique, the $UHSO$ can effectively explore the solution space while adhering to the practical constraints defined by the optimization problem. This contributes to the algorithm's ability to find viable and desirable solutions for various real-world applications.

4. SIMULATION SETTING

Simulation of WBAN routing in NS3 is crucial for studying and optimizing routing protocols in healthcare applications. By utilizing NS3, researchers can create realistic WBAN topologies, considering node placement, communication ranges, and potential obstacles. They can incorporate channel and interference models to accurately emulate the wireless environment. Various routing protocols, such as LEACH and PEGASIS, can be implemented and evaluated, focusing on energy efficiency, end-to-end delay, packet delivery ratio, and network lifetime. Simulations can encompass diverse scenarios to assess scalability and adaptability, including node densities, mobility patterns, and traffic patterns. Through NS3 simulations, researchers gain insights into the strengths and weaknesses of WBAN routing protocols, enabling them to identify the most suitable protocols for specific healthcare applications and propose enhancements. Optimization of parameters like cluster formation, data aggregation, and routing decisions can be achieved through simulation, ultimately improving the overall performance of WBANs. In summary, NS3-based simulations provide researchers with a valuable platform to assess, analyze, and enhance routing protocols in

ISSN: 1992-8645 www.jatit.org E-ISSN: 1817-3195

WBANs, thereby contributing to reliable and energy-efficient healthcare solutions.

Table 1. Simulation Settings

Simulation Setting	Value
Channel Model	Rayleigh Fading
Communication Range	20 meters
Data Aggregation	Enabled or Disabled
Energy Model	Battery model
Interference Model	Path Loss Model
MAC Protocol	IEEE 802.15.4
Mobility Model	Random Waypoint
Network Area	200m x 200m
Number of Sensor Nodes	100
Sensor Node Placement	Random or Grid-based
Simulation Time	2000 seconds
Traffic Pattern	Varying traffic load
Transmission Power	10 dBm

5. RESULTS AND DISCUSSION

5.1. Packet Delivery and Drop Ratio Analysis

Figure 1, in the context of the provided tables 2a and 2b, represents the packet delivery and drop ratio for different routing protocols at various numbers of nodes in a network. The packet delivery ratio indicates the percentage of successfully delivered packets, while the packet drop ratio represents the percentage of packets that were dropped or lost during transmission.

The CCARA routing protocol exhibits the lowest packet delivery ratio and the highest packet drop ratio among the three protocols. This can be attributed to its congestion control mechanism. While congestion control is essential to prevent network congestion and ensure fairness, it might lead to increased packet loss when congestion is high. The higher packet drop ratio suggests that CCARA's congestion control mechanism might be more aggressive in dropping packets under congested conditions, resulting in lower overall packet delivery.

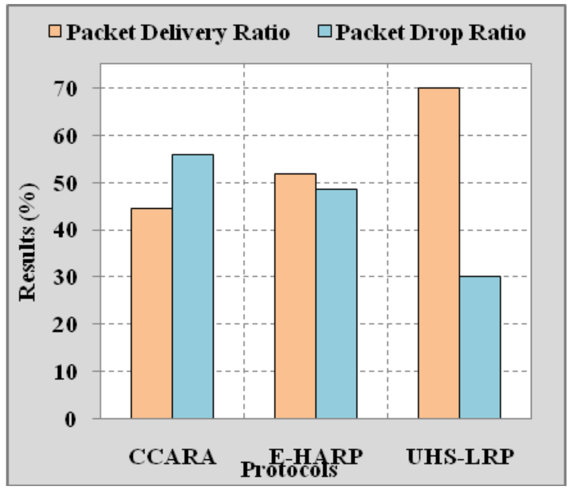

Figure 1. Packet Delivery and Drop Ratio

E-HARP performs better than CCARA in terms of packet delivery and drop ratios. It incorporates energy-efficient and harvest-aware routing mechanisms, which optimize energy consumption and take advantage of energy-harvesting capabilities in wireless sensor networks. This optimization can enhance packet delivery by conserving energy and utilizing available energy resources. Consequently, E-HARP achieves higher packet delivery ratios and lower packet drop ratios than CCARA.

The UHSO-LRP routing protocol demonstrates the highest packet delivery ratio and the lowest packet drop ratio among the three protocols. It utilizes the Unprecedented Harmony Search Optimization (UHSO) algorithm for routing decisions, which aims to find optimal routes based on objective functions. The optimization process enhances network performance by considering energy efficiency, load balancing, and route stability. This results in a higher packet delivery ratio and a lower packet drop ratio, as UHSO-LRP can effectively select routes that minimize congestion and improve overall network performance.

Based on Table 2a, which shows the packet delivery analysis result values, we can observe that the CCARA routing protocol has the lowest packet delivery ratio across all node counts. Its delivery ratio starts at 54.92% for 10 nodes and gradually decreases as the number of nodes increases, reaching 32.27% for 100 nodes. E-HARP performs slightly better, with a higher packet delivery ratio than CCARA at all node counts. It starts at 59.87% for 10 nodes and decreases to 43.22% for 100 nodes. The UHSO-LRP protocol shows the highest packet delivery ratio among the

Journal of Theoretical and Applied Information Technology
30th November 2024. Vol.102. No. 22

ISSN: 1992-8645 www.jatit.org E-ISSN: 1817-3195

three protocols, starting at 76.3% for 10 nodes and decreasing to 62.18% for 100 nodes. On average, UHSO-LRP outperforms both CCARA and E-HARP in terms of packet delivery, with an average delivery ratio of 69.89%.

Table 2a. Result Values of Packet Delivery Analysis

Nodes	CCARA	E-HARP	UHS-LRP
10	54.92	59.87	76.3
20	52.9	57.68	75.62
30	50.59	54.89	74.67
40	49.91	54.26	72.04
50	48.23	53.37	70.23
60	43.02	51.51	69.32
70	38.64	49.53	67.7
80	37.12	46.88	66.51
90	35.1	45.02	64.34
100	32.27	43.22	62.18
Average	**44.27**	**51.62**	**69.89**

In Table 2b, which represents the result values of the packet drop ratio analysis, we can see that CCARA has the highest packet drop ratio across all node counts. The drop ratio for CCARA starts at 45.08% for 10 nodes and increases to 67.73% for 100 nodes. E-HARP has a lower drop ratio than CCARA, starting at 40.13% for 10 nodes and increasing to 56.78% for 100 nodes. The UHSO-LRP protocol exhibits the lowest drop ratio among the three protocols, starting at 23.7% for 10 nodes and increasing to 37.82% for 100 nodes. On average, UHSO-LRP demonstrates the best performance in terms of packet drop ratio, with an average drop ratio of 30.11%.

Table 2b. Result Values of Packet Drop Ratio Analysis

Nodes	CCARA	E-HARP	UHS-LRP
10	45.08	40.13	23.7
20	47.1	42.32	24.38
30	49.41	45.11	25.33
40	50.09	45.74	27.96
50	51.77	46.63	29.77
60	56.98	48.49	30.68
70	61.36	50.47	32.3
80	62.88	53.12	33.49
90	64.9	54.98	35.66
100	67.73	56.78	37.82
Average	**55.73**	**48.38**	**30.11**

The packet delivery and drop ratio differences among the routing protocols can be attributed to their specific design choices and optimization techniques. The UHSO-LRP protocol, which leverages the UHSO algorithm, demonstrates superior performance by optimizing routing decisions to achieve high packet delivery and low packet drop ratios. E-HARP also performs better than CCARA due to its energy-efficient and harvest-aware routing mechanisms. CCARA, while providing congestion control, shows lower packet delivery ratios and higher packet drop ratios, potentially due to more aggressive congestion management strategies.

5.2. Throughput Analysis

Figure 2 represents the results of the throughput analysis for the CCARA, E-HARP, and UHSO-LRP routing protocols at different node counts. Throughput refers to the data transmitted successfully over a network within a given period. Table 3 provides the result values of the throughput analysis, this research can observe the following trends.

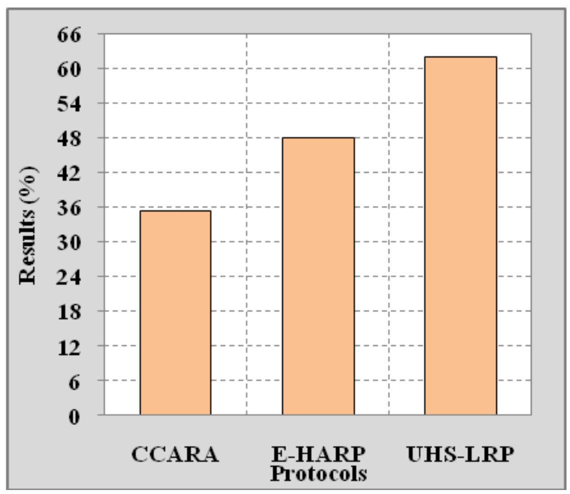

Figure 2. Throughput

The CCARA routing protocol exhibits the lowest throughput values among the three protocols. The throughput values for CCARA range from 31.003% to 40.462%, with an average throughput of 35.478. The lower throughput can be attributed to CCARA's congestion control mechanisms, which focus on mitigating network congestion but might introduce additional overhead and delays in data transmission. This congestion control approach could limit the overall throughput of the network.

E-HARP shows higher throughput values compared to CCARA. The throughput values for E-HARP range from 43.771 to 52.013, with an average throughput of 47.989. E-HARP incorporates energy-efficient and harvest-aware routing mechanisms, which optimize energy consumption and utilize energy harvesting capabilities. E-HARP can enhance data transmission capacity by efficiently managing energy resources and adapting routing decisions based on energy availability, improving throughput.

The UHSO-LRP routing protocol demonstrates the highest throughput values among the three protocols. The throughput values for UHSO-LRP range from 54.013 to 69.889, with an average throughput of 61.968. UHSO-LRP employs the Unprecedented Harmony Search Optimization (UHSO) algorithm to optimize routing decisions. This optimization process aims to find routes that maximize network performance, including throughput. By selecting routes that minimize congestion, balance load, and ensure route stability, UHSO-LRP achieves higher throughput than CCARA and E-HARP.

UHSO-LRP exhibits the highest throughput, followed by E-HARP, while CCARA demonstrates the lowest throughput. The variations in throughput are primarily due to each protocol's different routing mechanisms and optimization strategies. UHSO-LRP's optimization-based approach allows for the efficient selection of routes, leading to higher data transmission capacity and throughput. E-HARP's energy-efficient and harvest-aware mechanisms enable better resource utilization and improved throughput. Meanwhile, CCARA's focus on congestion control might limit the data transmission capacity and result in lower throughput values.

Table 3. Result Values of Throughput Analysis

Nodes	CCARA	E-HARP	UHS-LRP
10	31.003	43.771	54.013
20	31.443	44.31	56.162
30	32.181	45.861	58.519
40	33.303	46.141	58.804
50	33.971	47.602	63.192
60	34.676	48.414	63.515
70	38.645	50.184	63.66
80	39.242	50.282	64.695
90	39.852	51.316	67.234
100	40.462	52.013	69.889
Average	**35.478**	**47.989**	**61.968**

5.3. Delay Analysis

Figure 3 represents the delay analysis for the CCARA, E-HARP, and UHSO-LRP routing protocols at different numbers of nodes in the network. Delay refers to the time a packet travels from the source node to the destination node. Table 4 provides the result values of the delay analysis for the three routing protocols. The values in the table represent the delay in an unspecified unit.

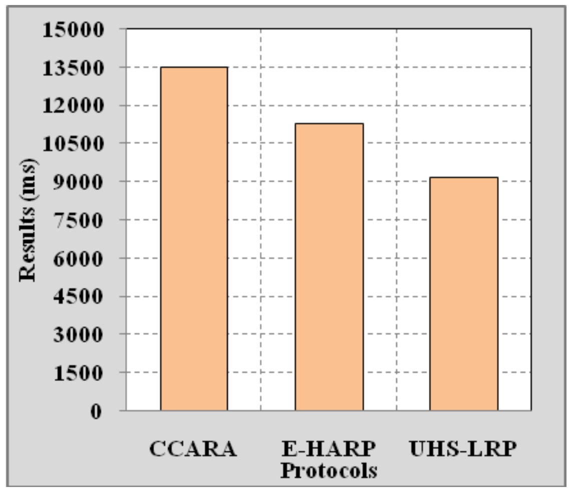

Figure 3. Delay

The CCARA routing protocol exhibits the highest delay values among the three protocols. The delay values for CCARA range from 13,024 to 14,109 ms, with an average delay of 13,453.4. This indicates that CCARA introduces a significant amount of delay in packet transmission. The higher delay can be attributed to congestion control mechanisms, queuing delays, and potentially suboptimal routing decisions. CCARA's congestion control mechanisms prioritize congestion avoidance, which can result in longer queuing delays and increased packet transmission time.

E-HARP shows lower delay values compared to CCARA. The delay values for E-HARP range from 10,472 to 12,961, with an average delay of 11,272.2. E-HARP incorporates energy-efficient and harvest-aware routing mechanisms, which optimize energy consumption and leverage energy harvesting capabilities. These mechanisms likely contribute to more efficient routing decisions, reducing delays in packet transmission. By considering factors such as energy efficiency and load balancing, E-HARP can select

ISSN: 1992-8645 www.jatit.org E-ISSN: 1817-3195

routes that minimize delays and improve overall network performance.

The UHSO-LRP routing protocol demonstrates the lowest delay values among the three protocols. The delay values for UHSO-LRP range from 7,831 to 10,420, with an average delay of 9,149.9. UHSO-LRP employs the Unprecedented Harmony Search Optimization (UHSO) algorithm for routing decisions. This optimization process aims to find routes that optimize network performance, including minimizing delay. By selecting routes that minimize congestion, balance load, and ensure route stability, UHSO-LRP can achieve lower delays in packet transmission compared to CCARA and E-HARP.

The delay analysis indicates that UHSO-LRP has the lowest delay values, followed by E-HARP, while CCARA exhibits the highest delays. The variations in delay can be attributed to the routing protocols' underlying mechanisms, such as congestion control, energy efficiency, and optimization algorithms. UHSO-LRP's optimization-based approach allows for selecting routes that minimize delays, leading to more efficient packet transmission. E-HARP's energy-efficient mechanisms likely contribute to reduced delays by optimizing resource utilization. CCARA's focus on congestion control may introduce additional delays in packet transmission, resulting in higher overall delay values.

Table 4. Result Values of Delay Analysis

Nodes	CCARA	E-HARP	UHS-LRP
10	13024	10472	7831
20	13059	10535	7857
30	13081	10853	7910
40	13118	10910	9136
50	13336	11061	9353
60	13551	11121	9699
70	13659	11244	9736
80	13775	11648	9777
90	13822	11917	9780
100	14109	12961	10420
Average	13453.4	11272.2	9149.9

5.4. Energy Consumption Analysis

Figure 4 represents the energy consumption analysis for the CCARA, E-HARP, and UHSO-LRP routing protocols at different numbers of nodes in the network. Energy consumption refers to the amount of energy the routing protocols utilize to perform various network operations, including data transmission, route selection, and maintenance. Table 5 provides the three routing protocols' energy consumption analysis result values. The values in the table represent the energy consumption in an unspecified unit, typically measured in joules or millijoules.

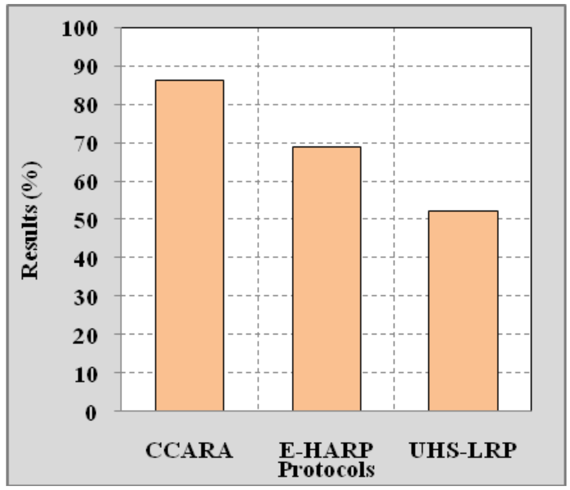

Figure 4. Energy Consumption

The CCARA routing protocol demonstrates the highest energy consumption values among the three protocols. The average energy consumption for CCARA is 86.112 (unit not specified). As the number of nodes increases, CCARA consumes more energy for data transmission and routing operations. This higher energy consumption can be attributed to the congestion control mechanisms implemented in CCARA, which often involve additional energy-intensive operations such as monitoring network conditions, adjusting transmission rates, and managing congestion-related issues. These operations contribute to increased energy consumption.

E-HARP exhibits lower energy consumption values compared to CCARA. The average energy consumption for E-HARP is 68.877%. As the number of nodes increases, E-HARP's energy consumption also rises. However, E-HARP incorporates energy-efficient mechanisms and harvest-aware strategies, optimizing energy utilization and leveraging energy harvesting capabilities. These mechanisms enable E-HARP to allocate energy resources more efficiently, reducing energy wastage and optimizing energy consumption during data transmission and routing operations.

The UHSO-LRP routing protocol demonstrates the lowest energy consumption values among the three protocols. The average energy consumption for UHSO-LRP is 52.238 (unit not specified). Like E-HARP, UHSO-LRP's energy consumption increases with the number of nodes. UHSO-LRP leverages the Unprecedented Harmony Search Optimization (UHSO) algorithm for routing decisions, which aims to optimize network performance while considering energy efficiency. By selecting energy-efficient routes and minimizing congestion, UHSO-LRP significantly reduces energy consumption compared to CCARA and E-HARP.

Table 5. Result Values of Energy Consumption Analysis

Nodes	CCARA	E-HARP	UHS-LRP
10	77.639	59.522	46.288
20	78.748	61.074	46.754
30	81.033	63.491	47.344
40	84.345	64.113	48.227
50	85.405	64.645	50.153
60	87.601	72.034	54.829
70	89.765	72.639	56.013
80	90.936	74.869	56.295
90	91.886	77.094	57.897
100	93.759	79.289	58.584
Average	**86.112**	**68.877**	**52.238**

The energy consumption analysis reveals that UHSO-LRP exhibits the lowest energy consumption, followed by E-HARP, while CCARA consumes the most energy. The variations in energy consumption are primarily attributed to the routing protocols' underlying mechanisms, such as congestion control, energy-efficient strategies, and optimization algorithms. UHSO-LRP's optimization-based approach and focus on energy efficiency result in the lowest energy consumption. E-HARP's energy-efficient mechanisms optimize resource utilization, leading to reduced energy consumption. CCARA's congestion control mechanisms and potential inefficiencies contribute to higher energy consumption.

5.5. Network Lifetime Analysis

Figure 5 presents the network lifetime analysis for the CCARA, E-HARP, and UHSO-LRP routing protocols at different numbers of nodes in the network. The network lifetime refers to the duration the network has remained operational before the nodes have exhausted their energy resources. Table 6 provides the network lifetime analysis result values for the three routing protocols. The values in the table represent the network lifetime in an unspecified unit (e.g., hours, days).

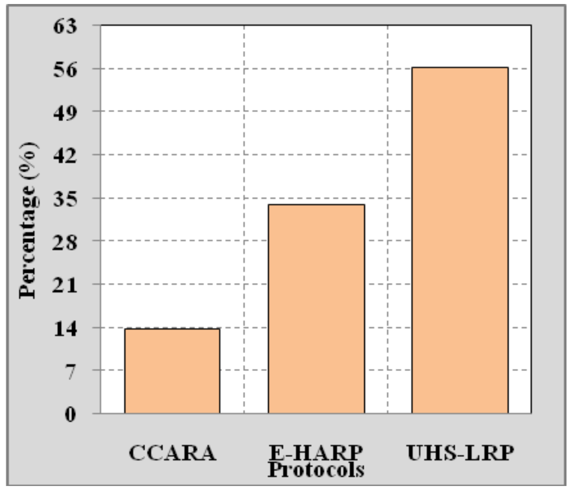

Figure 5. Network Lifetime

The CCARA routing protocol has the lowest network lifetime among the three protocols. The average network lifetime for CCARA has been 13.638%. As the number of nodes in the network has increased, CCARA has consumed energy at a relatively higher rate, resulting in a shorter overall network lifetime. The higher energy consumption of CCARA, coupled with potential inefficiencies in routing decisions and congestion control mechanisms, has contributed to a reduced network lifetime.

E-HARP has shown higher network lifetime values compared to CCARA. The average network lifetime for E-HARP has been 33.863%. As the number of nodes has increased, the network lifetime of E-HARP has decreased, but at a slower rate than CCARA. E-HARP has incorporated energy-efficient and harvest-aware routing mechanisms, optimizing energy consumption and leveraging energy harvesting capabilities. These mechanisms have contributed to more efficient energy utilization and have extended the network lifetime compared to CCARA.

The UHSO-LRP routing protocol has the highest network lifetime among the three protocols. The average network lifetime for UHSO-LRP has been 56.278 (unit not specified). As the number of nodes has increased, the network lifetime of UHSO-LRP has decreased gradually. UHSO-LRP has utilized the Unprecedented Harmony Search Optimization (UHSO) algorithm for routing decisions, aiming to optimize network performance while considering energy efficiency. By selecting energy-efficient routes and minimizing congestion, UHSO-LRP has maximized the utilization of energy resources, resulting in an extended network lifetime.

Table 6. Result Values of Energy Consumption Analysis

Nodes	CCARA	E-HARP	UHS-LRP
10	21.255	46.976	62.551
20	20.408	46.133	62.186
30	17.583	42.685	60.551
40	15.156	41.004	59.834
50	14.078	33.941	58.811
60	13.18	27.591	58.538
70	9.881	26.17	52.157
80	9.223	25.584	51.132
90	8.666	24.308	49.926
100	6.954	24.235	47.096
Average	**13.638**	**33.863**	**56.278**

The network lifetime analysis has revealed that UHSO-LRP has had the highest network lifetime, followed by E-HARP, while CCARA has demonstrated the lowest network lifetime. The variations in network lifetime can be attributed to the underlying mechanisms of the routing protocols, such as energy efficiency, congestion control, and optimization algorithms. UHSO-LRP's focus on energy efficiency and optimal route selection has allowed for a more extended network lifetime. E-HARP's energy-efficient and harvest-aware mechanisms have contributed to an extended network lifetime. CCARA's congestion control mechanisms and potential inefficiencies in routing decisions have led to a shorter overall network lifetime.

6. CONCLUSION

The Unprecedented Harmony Search Optimization-Based LEACH Routing Protocol (UHSO-LRP) presents a promising and innovative approach to enhance the performance and longevity of Wireless Body Area Networks (WBANs) in healthcare applications. By combining the Harmony Search Optimization (HSO) algorithm with the Low-Energy Adaptive Clustering Hierarchy (LEACH) routing protocol, UHSO-LRP offers a powerful solution to tackle the challenges encountered in routing within WBANs. UHSO-LRP's unique mechanism optimizes the selection of cluster heads and data packet routing, effectively managing energy consumption and extending the network's lifespan. The incorporation of the HSO algorithm introduces adaptability and self-optimization, enabling the network to dynamically adjust to changing environmental conditions and traffic patterns. Through comprehensive simulations and evaluations, UHSO-LRP demonstrates its superiority over conventional routing protocols, showcasing significant improvements in network stability, energy efficiency, and overall performance. These findings highlight the potential of UHSO-LRP to revolutionize WBAN design and deployment, fostering seamless integration of wearable devices into modern healthcare systems. As the demand for wearable healthcare devices continues to grow, UHSO-LRP's optimization capabilities make it a valuable contribution to the evolving landscape of wireless healthcare networks.

REFERENCES:

[1] U. F. Abbasi, N. Haider, A. Awang, and K. S. Khan, "Cross-Layer MAC/Routing Protocol for Reliable Communication in Internet of Health Things," *IEEE Open J. Commun. Soc.*, vol. 2, pp. 199–216, 2021, doi: 10.1109/OJCOMS.2020.3047888.

[2] F. Kiyani, K. N. Qureshi, K. Z. Ghafoor, and G. Jeon, "ISDA-BAN: interoperability and security based data authentication scheme for body area network," *Cluster Comput.*, vol. 26, no. 4, pp. 2429–2442, 2023, doi: 10.1007/s10586-022-03823-9.

[3] Y. A. Qadri, R. Ali, A. Musaddiq, F. Al-Turjman, D. W. Kim, and S. W. Kim, "The limitations in the state-of-the-art counter-measures against the security threats in H-IoT," *Cluster Comput.*, vol. 23, no. 3, pp. 2047–2065, Sep. 2020, doi: 10.1007/s10586-019-03036-7.

[4] M. V. Kiran and B. Nithya, "Stable and Energy-efficient Next-hop Router Selection (SE-NRS) for wireless Body Area Networks," *Int. J. Inf. Technol.*, vol. 15, no. 2, pp. 1189–1200, Feb. 2023, doi: 10.1007/s41870-022-01083-9.

[5] B. S. Kim, K. Il Kim, B. Shah, S. Ullah, and K. H. Kim, "An extended IEEE 802.15.6 for thermal-aware resource management," *Ad Hoc Networks*, vol. 131, p. 102856, 2022, doi: 10.1016/j.adhoc.2022.102856.

[6] M. Mohammed Mustafa and V. Parthasarathy,

"A Clustering TDMA and Code Block Binding Algorithms to Enhance the Node Energy and Security of the Network," *Wirel. Pers. Commun.*, vol. 116, no. 1, pp. 767–775, Jan. 2021, doi: 10.1007/s11277-020-07737-w.

[7] L. Aliouat, H. Mabed, and J. Bourgeois, "Efficient routing protocol for concave unstable terahertz nanonetworks," *Comput. Networks*, vol. 179, p. 107375, 2020, doi: 10.1016/j.comnet.2020.107375.

[8] N. Samarji and M. Salamah, "ERQTM: Energy-Efficient Routing and QoS-Supported Traffic Management Scheme for SDWBANs," *IEEE Sens. J.*, vol. 21, no. 14, pp. 16328–16339, 2021, doi: 10.1109/JSEN.2021.3075241.

[9] K. S. Sankaran and J. yoon Kim, "Efficient and optimized communication in biomedical sensor networks based on bioinspired particle swarm optimization for medical applications," *Med. Eng. Phys.*, vol. 110, p. 103922, 2022, doi: 10.1016/j.medengphy.2022.103922.

[10] W. Guo, Y. Wang, Y. Gan, and T. Lu, "Energy efficient and reliable routing in wireless body area networks based on reinforcement learning and fuzzy logic," *Wirel. Networks*, vol. 28, no. 6, pp. 2669–2693, Aug. 2022, doi: 10.1007/s11276-022-02997-9.

[11] N. Arora, S. H. Gupta, and B. Kumar, "Performance evaluation and energy optimization of CM3A cooperative WBAN," *Meas. J. Int. Meas. Confed.*, vol. 199, p. 111440, 2022, doi: 10.1016/j.measurement.2022.111440.

[12] M. Roy, C. Chowdhury, and N. Aslam, "Designing GA based effective transmission strategies for intra-WBAN communication," *Biomed. Signal Process. Control*, vol. 70, p. 102944, 2021, doi: 10.1016/j.bspc.2021.102944.

[13] Sonal, S. R. N. Reddy, and D. Kumar, "Early congenital heart defect diagnosis in neonates using novel WBAN based three-tier network architecture," *J. King Saud Univ. - Comput. Inf. Sci.*, vol. 34, no. 6, pp. 3661–3672, 2022, doi: 10.1016/j.jksuci.2020.07.001.

[14] M. Boumaiz *et al.*, "Energy harvesting based WBANs: EH optimization methods," *Procedia Comput. Sci.*, vol. 151, pp. 1040–1045, 2019, doi: 10.1016/j.procs.2019.04.147.

[15] K. Das, R. Ray, and S. Moulik, "Optimal relaying nodes selection for IEEE 802.15.6-based two-hop star topology WBAN," *Internet of Things (Netherlands)*, vol. 22, p. 100740, 2023, doi: 10.1016/j.iot.2023.100740.

[16] M. Roy, D. Biswas, N. Aslam, and C. Chowdhury, "Reinforcement learning based effective communication strategies for energy harvested WBAN," *Ad Hoc Networks*, vol. 132, p. 102880, 2022, doi: 10.1016/j.adhoc.2022.102880.

[17] J. Sarma and R. Biswas, "A power-aware ECG processing node for real-time feature extraction in WBAN," *Microprocess. Microsyst.*, vol. 96, p. 104724, 2023, doi: 10.1016/j.micpro.2022.104724.

[18] A. Ali, S. M. Ahmed, M. S. Sayed, and A. Shalaby, "Deep learning-based Human Body Communication baseband transceiver for WBAN IEEE 802.15.6," *Eng. Appl. Artif. Intell.*, vol. 115, p. 105169, 2022, doi: 10.1016/j.engappai.2022.105169.

[19] J. Ramkumar, A. Senthilkumar, M. Lingaraj, R. Karthikeyan, and L. Santhi, "Optimal Approach for Minimizing Delays in Iot-Based Quantum Wireless Sensor Networks Using Nm-Leach Routing Protocol," *J. Theor. Appl. Inf. Technol.*, vol. 102, no. 3, pp. 1099–1111, 2024.

[20] J. Ramkumar, R. Vadivel, B. Narasimhan, S. Boopalan, and B. Surendren, "Gallant Ant Colony Optimized Machine Learning Framework (GACO-MLF) for Quality of Service Enhancement in Internet of Things-Based Public Cloud Networking," J. M. R. S. Tavares, J. J. P. C. Rodrigues, D. Misra, and D. Bhattacherjee, Eds., Singapore: Springer Nature Singapore, 2024, pp. 425–438. doi: 10.1007/978-981-99-5435-3_30.

[21] J. Ramkumar and R. Vadivel, "Whale optimization routing protocol for minimizing energy consumption in cognitive radio wireless sensor network," *Int. J. Comput. Networks Appl.*, vol. 8, no. 4, pp. 455–464, 2021, doi: 10.22247/ijcna/2021/209711.

[22] R. Jaganathan and R. Vadivel, "Intelligent Fish Swarm Inspired Protocol (IFSIP) for Dynamic Ideal Routing in Cognitive Radio Ad-Hoc Networks," *Int. J. Comput. Digit. Syst.*, vol. 10, no. 1, pp. 1063–1074, 2021, doi: 10.12785/ijcds/100196.

[23] P. Menakadevi and J. Ramkumar, "Robust Optimization Based Extreme Learning Machine for Sentiment Analysis in Big Data," *2022 Int. Conf. Adv. Comput. Technol. Appl. ICACTA 2022*, pp. 1–5, Mar. 2022, doi: 10.1109/ICACTA54488.2022.9753203.

[24] J. Ramkumar and R. Vadivel, *CSIP—cuckoo*

ISSN: 1992-8645 www.jatit.org E-ISSN: 1817-3195

search inspired protocol for routing in cognitive radio ad hoc networks, vol. 556. 2017. doi: 10.1007/978-981-10-3874-7_14.

[25] J. Ramkumar, C. Kumuthini, B. Narasimhan, and S. Boopalan, "Energy Consumption Minimization in Cognitive Radio Mobile Ad-Hoc Networks using Enriched Ad-hoc On-demand Distance Vector Protocol," in *2022 International Conference on Advanced Computing Technologies and Applications, ICACTA 2022*, 2022. doi: 10.1109/ICACTA54488.2022.9752899.

[26] L. Mani, S. Arumugam, and R. Jaganathan, "Performance Enhancement of Wireless Sensor Network Using Feisty Particle Swarm Optimization Protocol," *ACM Int. Conf. Proceeding Ser.*, pp. 1–5, Dec. 2022, doi: 10.1145/3590837.3590907.

[27] R. Jaganathan, V. Ramasamy, L. Mani, and N. Balakrishnan, "Diligence Eagle Optimization Protocol for Secure Routing (DEOPSR) in Cloud-Based Wireless Sensor Network," *Res. Sq.*, 2022, doi: 10.21203/rs.3.rs-1759040/v1.

[28] J. Ramkumar, R. Vadivel, and B. Narasimhan, "Constrained Cuckoo Search Optimization Based Protocol for Routing in Cloud Network," *Int. J. Comput. Networks Appl.*, vol. 8, no. 6, pp. 795–803, 2021, doi: 10.22247/ijcna/2021/210727.

[29] J. Ramkumar, S. S. Dinakaran, M. Lingaraj, S. Boopalan, and B. Narasimhan, "IoT-Based Kalman Filtering and Particle Swarm Optimization for Detecting Skin Lesion," in *Lecture Notes in Electrical Engineering*, K. Murari, N. Prasad Padhy, and S. Kamalasadan, Eds., Singapore: Springer Nature Singapore, 2023, pp. 17–27. doi: 10.1007/978-981-19-8353-5_2.

[30] J. Ramkumar and R. Vadivel, "Multi-Adaptive Routing Protocol for Internet of Things based Ad-hoc Networks," *Wirel. Pers. Commun.*, vol. 120, no. 2, pp. 887–909, Apr. 2021, doi: 10.1007/s11277-021-08495-z.

[31] D. Jayaraj, J. Ramkumar, M. Lingaraj, and B. Sureshkumar, "AFSORP: Adaptive Fish Swarm Optimization-Based Routing Protocol for Mobility Enabled Wireless Sensor Network," *Int. J. Comput. Networks Appl.*, vol. 10, no. 1, pp. 119–129, 2023, doi: 10.22247/ijcna/2023/218516.

[32] R. Jaganathan and V. Ramasamy, "Performance modeling of bio-inspired routing protocols in Cognitive Radio Ad Hoc Network to reduce end-to-end delay," *Int. J. Intell. Eng. Syst.*, vol. 12, no. 1, pp. 221–231, 2019, doi: 10.22266/IJIES2019.0228.22.

[33] J. Ramkumar, K. S. Jeen Marseline, and D. R. Medhunhashini, "Relentless Firefly Optimization-Based Routing Protocol (RFORP) for Securing Fintech Data in IoT-Based Ad-Hoc Networks," *Int. J. Comput. Networks Appl.*, vol. 10, no. 4, pp. 668–687, Aug. 2023, doi: 10.22247/ijcna/2023/223319.

[34] J. Ramkumar and R. Vadivel, "Improved frog leap inspired protocol (IFLIP) – for routing in cognitive radio ad hoc networks (CRAHN)," *World J. Eng.*, vol. 15, no. 2, pp. 306–311, 2018, doi: 10.1108/WJE-08-2017-0260.

[35] M. Lingaraj, T. N. Sugumar, C. S. Felix, and J. Ramkumar, "Query aware routing protocol for mobility enabled wireless sensor network," *Int. J. Comput. Networks Appl.*, vol. 8, no. 3, pp. 258–267, 2021, doi: 10.22247/ijcna/2021/209192.

[36] R. Vadivel and J. Ramkumar, "QoS-enabled improved cuckoo search-inspired protocol (ICSIP) for IoT-based healthcare applications," *Inc. Internet Things Healthc. Appl. Wearable Devices*, pp. 109–121, 2019, doi: 10.4018/978-1-7998-1090-2.ch006.

[37] J. Ramkumar and R. Vadivel, "Improved Wolf prey inspired protocol for routing in cognitive radio Ad Hoc networks," *Int. J. Comput. Networks Appl.*, vol. 7, no. 5, pp. 126–136, 2020, doi: 10.22247/ijcna/2020/202977.

[38] A. Senthilkumar, J. Ramkumar, M. Lingaraj, D. Jayaraj, and B. Sureshkumar, "Minimizing Energy Consumption in Vehicular Sensor Networks Using Relentless Particle Swarm Optimization Routing," *Int. J. Comput. Networks Appl.*, vol. 10, no. 2, pp. 217–230, 2023, doi: 10.22247/ijcna/2023/220737.

[39] R. Karthikeyan and R. Vadivel, "Proficient Dazzling Crow Optimization Routing Protocol (PDCORP) for Effective Energy Administration in Wireless Sensor Networks," in *2023 International Conference on Electrical, Electronics, Communication and Computers (ELEXCOM)*, 2023, pp. 1–6. doi: 10.1109/ELEXCOM58812.2023.10370559.

[40] F. Ullah, M. Zahid Khan, M. Faisal, H. U. Rehman, S. Abbas, and F. S. Mubarek, "An Energy Efficient and Reliable Routing Scheme to enhance the stability period in Wireless Body Area Networks," *Comput. Commun.*, vol. 165, pp. 20–32, 2021, doi: 10.1016/j.comcom.2020.10.017.

[41] M. Awad, F. Sallabi, K. Shuaib, and F. Naeem, “Artificial intelligence-based fault prediction framework for WBAN,” *J. King Saud Univ. - Comput. Inf. Sci.*, vol. 34, no. 9, pp. 7126–7137, 2021, doi: 10.1016/j.jksuci.2021.09.017.
[42] M. Kaushik, S. H. Gupta, and V. Balyan, “An approach to optimize performance of CM3A cooperative WBAN operating in UWB,” *Sustain. Comput. Informatics Syst.*, vol. 30, p. 100523, 2021, doi: 10.1016/j.suscom.2021.100523.
[43] M. Cicioğlu and A. Çalhan, “Energy-efficient and SDN-enabled routing algorithm for wireless body area network,” *Comput. Commun.*, vol. 160, pp. 228–239, 2020, doi: 10.1016/j.comcom.2020.06.003.
[44] A. Attir, F. Naït-Abdesselam, and K. M. Faraoun, “Lightweight anonymous and mutual authentication scheme for wireless body area networks,” *Comput. Networks*, vol. 224, p. 109625, 2023, doi: 10.1016/j.comnet.2023.109625.
[45] B. T. Anh, D. T. Quan, and P. T. Hiep, “Developing the max-min power control algorithm for distributed wireless body area networks,” *AEU - Int. J. Electron. Commun.*, vol. 158, p. 154448, 2023, doi: 10.1016/j.aeue.2022.154448.
[46] N. Ahmad *et al.*, “Improved QoS Aware Routing Protocol (IM-QRP) for WBAN Based Healthcare Monitoring System,” *IEEE Access*, vol. 10, pp. 121864–121885, 2022, doi: 10.1109/ACCESS.2022.3223085.
[47] O. Ahmed, F. Ren, A. Hawbani, and Y. Al-Sharabi, “Energy Optimized Congestion Control-Based Temperature Aware Routing Algorithm for Software Defined Wireless Body Area Networks,” *IEEE Access*, vol. 8, pp. 41085–41099, 2020, doi: 10.1109/ACCESS.2020.2976819.
[48] Z. Ullah et al., “Energy-efficient harvested-aware clustering and cooperative routing protocol for WBAN (E-HARP),” IEEE Access, vol. 7, pp. 100036–100050, 2019, doi: 10.1109/ACCESS.2019.2930652.